Conference Paper, Published Version

Schuppener, Bernd; Kauther, Regina; Kramer, Helmut; Vorbau, Jana

Ship collision with sloped banks of waterways - an approach to determining the stopping distance

31st PIANC Congress
Estoril, May 2006
Portugal

SHIP COLLISIONS WITH SLOPED BANKS OF WATERWAYS – AN APPROACH TO DETERMINING THE STOPPING DISTANCE

Bernd Schuppener, Regina Kauther, Federal Waterways Engineering and Research Institute, Karlsruhe, Germany
Helmut Kramer, Jana Vorbau, VBI Construction Engineering Consultants, Kramer + Albrecht, Hamburg

ABSTRACT

When ships collide with the sloped banks of waterways, the damage to revetments is usually limited. However, such collisions may impair the structural stability and serviceability of any structures such as bridge abutments located in the immediate vicinity of the bank. A set of formulae to forecast the impact and the stopping distance in the event of a collision was derived by Meier-Dörnberg (1983). The formulae are based on the principles of linear momentum and the conservation of angular momentum and assume that the bank is rigid. However, cases of damage have shown that ships always penetrate the slopes of waterways which are usually protected by revetments with riprap. This paper presents a forecast model which applies the law of conservation of energy and also takes into account the effect of the soil resistance when the bow of a ship penetrates a slope. Model tests and field tests conducted by the Federal Waterways Engineering and Research Institute (BAW) were performed to investigate the behaviour of the ground and the ship in the event of a collision. These tests were used to check the suitability of the two forecast models. The results of the tests and the forecasts are presented. It is shown that both models give conservative but realistic predictions of the stopping distance and the impact forces. This will provide the basis for a realistic assessment of the safety of structures built next to waterways in Germany.

KEYWORDS: ship collision, banks of waterways

1. THEORETICAL MODELLING OF A SHIP COLLISION

There are two ways of proceeding when calculating the displacements of the ship and the contact forces acting on the soil:

- The time-dependent displacements, $x(t)$ and $z(t)$, the velocities, rates of acceleration of the ship and the contact force, $F(t)$, between the slope and the bow of the ship can be calculated by establishing a kinematic equation, taking inertia into account.
- The components of the stopping distance, $s_{x,max}$ and $s_{z,max}$, of the ship can be calculated on the basis of the energy conservation law.

1.1. Method of calculation according to Meier-Dörnberg

Meier-Dörnberg (1983) developed a closed analytical solution to cover those cases in which the slope is rigid. In a collision with a rigid slope, the bow of the ship slides up the slope and then back down again if the collision takes place at an oblique angle.

The calculation method takes account of the entire spatial movement of the ship when it is being pushed up the slope, i. e. the translatory motion of its centre of gravity, $x(t)$, $y(t)$ and $z(t)$, and the rotation about the longitudinal axis (tilting), the vertical axis (change in the direction of travel) and the transverse axis (being pushed upwards), $\varphi_y(t)$. The calculation method has been considerably simplified by assuming that the edges of the bow are straight and that the surface of the sloping bank is both even and rigid. In addition, it is also assumed that both the ship and its cargo are rigid and that any deformations of the ship are taken into account at the point of impact only. The collision as a whole is divided into two phases:

- The first phase comprises the impact which deflects the tip of the bow and initiates the subsequent sliding movement. The new velocity components are determined after the impact, assuming that the impact is both rigid-plastic (the contact between the ship and the slope is maintained throughout the collision) and frictional. The same line of action is assumed for the Coulomb friction at the point of contact between the ship and the slope and for the velocity of the ship relative to the slope.
- The second phase covers the subsequent upward motion and deflection until the ship comes to a halt or moves down the slope again. The initial conditions for the velocities of the ship when it is pushed upwards are the final velocities calculated for the first phase. The values of the draught, buoyancy force and the buoyancy moment of the vessel, which change during the upward movement, are taken into account in the equations describing the motion of the ship.

When a vessel with mass, m, hits a sloping bank with an inclination, α, at right angles and at a velocity, v_a, the components of the stopping distance of the ship's centre of gravity, x_{max} and z_{max}, given a friction coefficient of $\tan\delta$ between the bow and the slope, are obtained from the differential equation describing the motion of the ship for $z(t)$ or $x(t)$ as follows:

$$z_{max} = \frac{v_a}{\omega} \cdot \left(\frac{\cot\alpha - \tan\delta}{\left(1 + \frac{\tan\delta}{\tan\alpha}\right) + a_j \left(\frac{1}{\tan^2\alpha} - \frac{\tan\delta}{\tan\alpha} \right)} \right)$$

with

$$a_j = 1 + \frac{a_x^2}{i_y^2}$$

where a_x is the distance between the point of contact between the bow and the slope and the centre of gravity of the ship, i_y is the radius of gyration about the y-axis and

$$\omega = \sqrt{\frac{g}{h_0}\left(1 - \left(\frac{(\cot\alpha - \tan\delta)\cdot\cot\alpha \cdot a_j}{\left(1 + \frac{\tan\delta}{\tan\alpha}\right) + a_j \left(\frac{1}{\tan^2\alpha} - \frac{\tan\delta}{\tan\alpha} \right)} \right)\right)}$$

in which g is the acceleration due to gravity and h_0 is the draught. The maximum vertical lift of the assumed point of contact is calculated as follows:

$$s_{z,max} = z_{max} \cdot a_j$$

The maximum horizontal force occurring at the end of the upward movement is:

$$F_{x,max} = \frac{g}{h_0} \cdot \frac{m \cdot a_j \cdot (\sin\alpha + \cos\alpha \cdot \tan\delta)}{(\sin\alpha \cdot \tan\delta + a_j \cos\alpha)} \cdot z_{max}$$

1.2 Modelling with the energy conservation law

Another way of describing the collision of a ship with a sloping bank is to apply the law of energy conservation. In this approach it is assumed that, on collision with the sloping bank, the kinetic energy, E_{kin}, of the ship is converted into

- frictional work, E_R, between the soil and the bow of the ship,
- potential energy, E_{pot}, due to the lifting of the bow during the collision,
- deformational work, E_{Ep}, of the passive resistance of the soil in front of the bow when the latter penetrates the slope and
- deformational work, E_{bow}, due to the crushing of the ship's bow :

$$E_{kin} = E_R + E_{pot} + E_{Ep} + E_{bow}$$

Compared with the method according to MEIER-DÖRNBERG, the advantage of this approach is that the work done by the resistance of the ground in front of the bow can be taken into account. The following sections show that the three energy components, E_R, E_{pot} and E_{Ep}, are dependent on the stopping distance, s_{max}.

1.2.1. Determination of the vertical components of the contact force between bow and slope

The contact force between the bow of the ship and the slope is used to calculate the frictional work and the potential energy. It can be determined from the equilibrium of the vertical forces acting on the ship. When the bow travels up the slope, an additional volume, ΔV_{bow}, emerges from the water while the stern simultaneously sinks deeper into the water, displacing an additional volume of water, ΔV_{stern}, (Figure 1). By way of simplification, the volume of the bow above the water and in front of the point of contact is disregarded and the hull is taken to be a rectangular parallelepiped of length, L, and width, B.

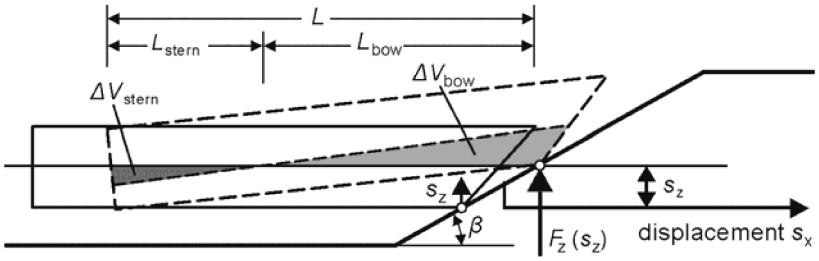

Figure 1: Geometrical quantities on collision of a pontoon-type bow with a sloping bank

Based on the equilibrium condition of the vertical forces, the following equation is obtained with the weight density of water, γ_W, and the vertical component, $F_z(s_z)$, of the contact force of the bow:

$$\Delta V_{stern} \cdot \gamma_W + F_z(s_z) = \Delta V_{bow} \cdot \gamma_W \quad (1)$$

The following equation is obtained from the sum of the moments about the point of contact at the bow:

$$\Delta V_{stern} \cdot \gamma_W \cdot (L_{bow} + 2/3 \cdot L_{stern}) = \Delta V_{bow} \cdot \gamma_W \cdot 1/3 \cdot L_{bow}$$
$$\Delta V_{stern} / \Delta V_{bow} = 1/3 \cdot L_{bow} / (L_{bow} + 2/3 \cdot L_{stern}) \quad (2)$$

In addition, the following apply to the simplified assumption that the hull is a rectangular parallelepiped of width, B:

$$L_{bow} + L_{stern} = L \quad (3)$$
$$\Delta V_{bow} = 0.5 \cdot s_z \cdot L_{bow} \cdot B \quad (4)$$
$$\Delta V_{stern} = 0.5 \cdot (L_{stern}/L_{bow}) \cdot s_z \cdot L_{stern} \cdot B \quad (5)$$

Thus there are five equations available for determining the five unknowns which are ΔV_{stern}, $F_z(s_z)$, ΔV_{bow}, L_{bow} and L_{stern}. After the appropriate transformation, $F_z(s_z)$ can be obtained as follows:

$$F_z(s_z) = s_z \cdot B \cdot \gamma_W \cdot L/4 \quad (6)$$

Assuming that a friction coefficient, tan δ, acts between the steel of the ship's bow and the soil of the slope when the bow travels up the slope and the upward path of the bow can be described by a straight line inclined at an angle, β, to the horizontal plane (Figure 2), the contact force is inclined by an angle, δ, to a line at right angles to the slope. Thus the contact force, $F(s_z)$, exerted on the slope by the bow is:

$$F(s_z) = F_z(s_z) / \cos(\beta + \delta) \quad (7)$$

and the frictional force, R, is:

$$R(s_z) = F \cdot \sin\delta = F_z(s_z) \cdot \sin\delta / \cos(\beta + \delta) \quad (8)$$

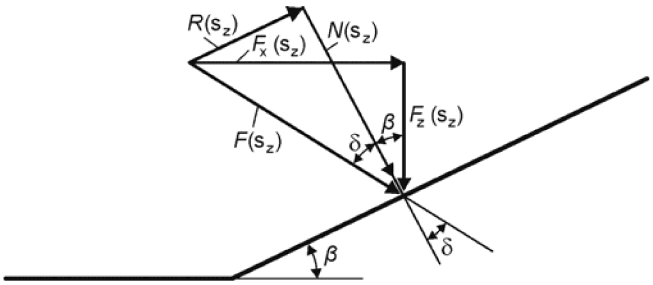

Figure 2: Assumptions and geometrical relationship between the contact force, F, and its components

It can be seen that the frictional force increases with s_z and therefore with the stopping distance, s_x, owing to the increase in the contact force. The ship is therefore increasingly slowed down as it travels up the slope.

1.2.2. Kinetic energy

The kinetic energy, E_{kin}, can be determined from the mass, m, of the ship and the collision velocity, v_a, as follows:

$$E_{kin} = m \cdot v_a^2 / 2$$

As the water exerts a pull on the ship during the collision, a hydrodynamic water mass of between 10 % and 20 % of the ship's mass is added to the kinetic energy of the ship.

1.2.3. Potential energy

The potential energy, E_{pot}, of the ship at the end point of the collision is the integral over the vertical component, $F_z(s_z)$, of the contact force from $s_z = 0$ to the maximum upward movement $s_z = s_{z,max}$, at which the ship comes to a halt. The following is obtained from (6):

$$E_{pot} = \int_{s_z=0}^{s_{z,max}} \gamma_w \cdot L/4 \cdot B \cdot s_z \cdot ds_z$$

$$E_{pot} = \gamma_W \cdot L/8 \cdot B \cdot s_{z,max}^2$$

with $s_z = s_x \cdot \tan \beta$:

$$E_{pot} = \gamma_W \cdot L/8 \cdot B \cdot \tan^2 \beta \cdot s_{x,max}^2 \quad (9)$$

It can be seen that the potential energy, E_{pot}, increases quadratically with the upward motion, s_z, of the bow and the stopping distance, $s_{x,max}$.

1.2.4. Frictional work of the contact force

Using (6) and (8), the frictional force as a function of the upward motion, s_z, of the bow can be determined as follows:

$$R(s_z) = s_z \cdot B \cdot \gamma_W \cdot L/4 \cdot \sin \delta / \cos (\beta + \delta)$$

and the frictional force as a function of the path, s, with $s_z = s \cdot \sin \beta$ is obtained as follows:

$$R(s_z) = s \cdot \sin \beta \cdot B \cdot \gamma_w \cdot L/4 \cdot \sin \delta / \cos (\beta + \delta)$$

The frictional work, E_R, done up to the point at which the ship comes to a halt is then the integral over the frictional force, $R(s_z)$, along the path from $s = 0$ to $s = s_{max}$ as follows:

$$E_R = \frac{\sin\beta \cdot \sin\delta}{4 \cdot \cos(\beta+\delta)} \cdot B \cdot \gamma_w \cdot L \int_{s=0}^{s_{max}} s \cdot ds$$

$$E_R = \frac{\sin\beta \cdot \sin\delta}{8 \cdot \cos(\beta+\delta)} \cdot B \cdot \gamma_w \cdot L \cdot s_{max}^2$$

Assuming that $s_{max} = s_{x,max}/\cos \beta$, the frictional work as a function of the horizontal component of the stopping distance, $s_{x,max}$, is:

$$E_R = \frac{\tan\beta \cdot \sin\delta}{8 \cdot \cos(\beta+\delta) \cdot \cos^2\beta} \cdot B \cdot \gamma_w \cdot L \cdot s_{x,max}^2 \quad (11)$$

It can be seen that the frictional energy, E_R, increases quadratically with the stopping distance.

1.2.5. Work of the passive earth pressure of the soil in front of the bow of the ship

The resistance of the slope to penetration by the ship is modelled with the passive earth pressure of the soil, cf. CALGARO (1991) and DENVER (1983). Closed solutions for the determination of the passive resistance of the soil in front of surfaces under pressure exist for straight surfaces only. However, the bow sections of ships with sharp

bows are generally curved. The geometry of the bow must therefore be approximated by means of straight surfaces to enable the passive earth pressure of the soil in front of the bow penetrating the slope to be determined. The geometry of the sliding wedge due to the passive resistance of the soil that occurs when a ship collides with a sloping bank at right angles is shown in Figure 3 for a simplified bow with two straight surfaces only.

When determining the work of the passive earth pressure of the soil, the lateral friction, R_0, of the wedge-shaped bodies causing the passive earth pressure of the soil is disregarded by way of simplification and only the horizontal component, E_{ph}, of the passive resistance of the soil and the friction at the ship's hull, R_s, mobilised by the passive resistance of the soil on penetration is taken into account..

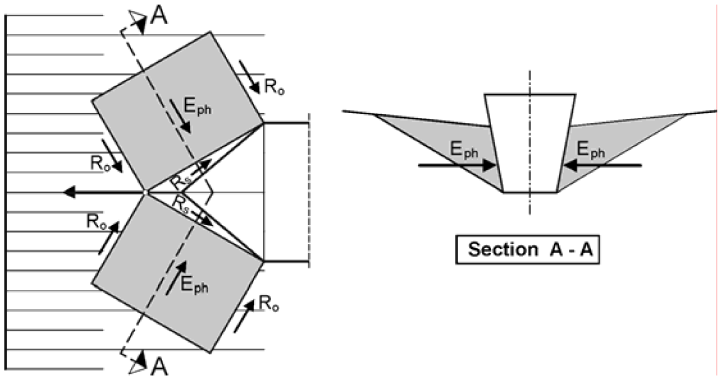

Figure 3: Sliding wedges causing the passive resistance of the soil, Eph, at the bow when a ship collides with a sloping bank at right angles and penetrates the slope horizontally

Unlike the vertical component of the contact force between the ship and the slope, the passive resistance of the soil in front of the bow is not a linear function of the path of the ship when it penetrates the slope. To calculate the work of the passive resistance of the soil, it is assumed that the ship penetrates the slope "step by step" (Figure 4). The components, E_{ph} and R_s, of the passive resistance of the soil and the work, E_{Ep}, done by the two components are then determined for each step. In doing so, it is taken into account that the passive resistance of the soil develops at an oblique angle to the inclination of the slope, i.e. the ground rises at an angle that is smaller than the angle of the slope, α.

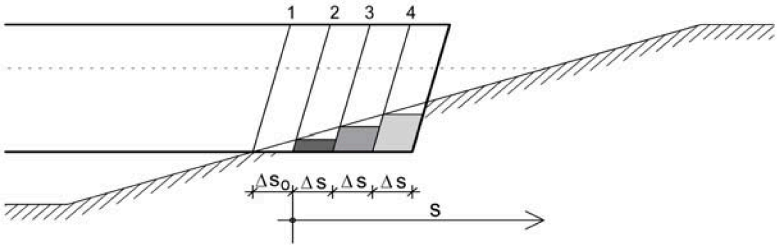

Figure 4: Step-by-step horizontal penetration into the sloping bank by the ship's bow for the determination of the work of the passive resistance of the soil

In the description of collisions by MEIER-DÖRNBERG (1983), the slope was assumed to be rigid. Under such conditions, the inclination, β, of the path of the point of contact corresponds to the angle of inclination, α, of the slope if the ship collides with the slope at right angles, i.e. when $\beta = \alpha$. When the bow penetrates the slope, $0 \leq \beta < \alpha$. In this case, the inclination, β, of the path of the point of contact is unknown. There are no other conditional equations for β. However, as there will be minimal soil resistance for the path occurring during a collision, the inclination, β, and thus the stopping distance can be determined by varying β. The decisive factor here is the inclination, β, of the path which results in the greatest stopping distance.

1.2.6. Stopping distance

It is possible to make an initial, quick and simple, if not always conservative, estimate of the stopping distance if the bank and the ship's bow are assumed to be rigid. In this case, the deformational work due to the crushing of the ship's bow and the passive resistance of the soil in front of the ship's bow is disregarded and the inclination, β, of the path of the point of contact is equal to the inclination of the slope, α, if the ship collides with the bank at right

angles. The kinetic energy is thus converted into potential energy and frictional work of the contact force between the ship's bow and the sloping bank, as follows:

$$E_{kin} = E_{pot}(s_{x.max}) + E_R(s_{x.max}) \quad (12)$$

With the kinetic energy:

$$E_{kin} = m \cdot v_a^2 / 2$$

of the potential energy (9) and the frictional energy (11), the horizontal component, $s_{x.max}$, of the stopping distance, taking (12) into account, is as follows:

$$s_{x,max} = v_a \sqrt{\frac{4 \cdot m}{\gamma_W \cdot L \cdot B \cdot \tan\alpha \cdot \left(\tan\alpha + \sin\delta / ((\cos(\alpha+\delta) \cdot \cos^2\alpha)\right)}}$$

It can be seen that a closed solution for the stopping distance, which increases linearly with the velocity of the ship on collision, is obtained under these conditions.

When taking into account the work of the passive resistance of the soil in front of the bow, the equation of the energy conservation law:

$$E_{kin} = E_R(s_{x.max}) + E_{pot}(s_{x.max}) + E_{Ep}(s_{x.max})$$

is best resolved iteratively in order to determine the stopping distance, $s_{x.max}$, because - as described in 1.2.5. – the work of the passive resistance of the soil has to be determined by assuming that the ship's bow penetrates the slope "step by step" and, furthermore, the relevant inclination of the inclination, β, of the path of the point of contact must be calculated by a variational calculation.

Whenever considerable deformations of the ship's bow occur, a further term for the deformational work at the ship's bow can be included in the equation. Initial approaches to determining the force-deformation relationship to be used in this case are stated in Part 9 of DIN 1055.

2. TESTS TO INVESTIGATE SHIP COLLISION

2.1. Introduction

First of all, small-scale model tests in dry sand were conducted, not only to verify the theoretical calculation methods but also to investigate the actual impact forces during ship collisions on waterways and the failures and deformations that occur. In addition, three field tests were performed to verify the results of the fifteen tests carried out in order to identify possible effects due to scale and any influence of the motion of the ship in the water as well as to investigate the magnitude and effect of pore water pressure in the soil during a collision. The investigations were limited to head-on collisions of typical loaded inland navigation vessels. The vessels were modelled as rigid bodies.

2.2. Model tests

2.2.1. Test set-up and procedure

The tests were performed in the test pit at the former Berlin office of the Federal Waterways Engineering and Research Institute. The model tests were designed with the aid of model laws which enabled the test results to be interpreted and the results of movement and force measurements in the model tests to be transposed to a large-scale prototype. The model of the slopes (Figure 5) is based on a cross-sectional profile of a sloping bank with a 1:3 gradient and a height of 5 m, which is common on federal waterways in Germany. The dry sand with a coefficient of uniformity, U, of around 2 was installed by pluviation. The in-situ density, D, was between 0.7 and 0.8. The sloping banks were modelled with a horizontal crest. The collision was applied in the centre of the test pit to ensure symmetrical conditions.

Two ships with bow designs typical of those used for inland navigation vessels, i.e. one with a sharp bow, the other with a pontoon-type bow, were selected for the model tests (Figure 6). A type IIa Europe barge, which has a width of 11.40 m and an overall length of 76.50 m, was chosen for the ship with a pontoon-type bow. The model tests were performed for a draught of 2.5 m, at which the ship has a tonnage of 1940 t. The *Johann Welker* type of vessel has a sharp bow and, with a width of 9.46 m and an overall length of 80.00 m, has a tonnage of 1611 t at a draught of 2.5 m.

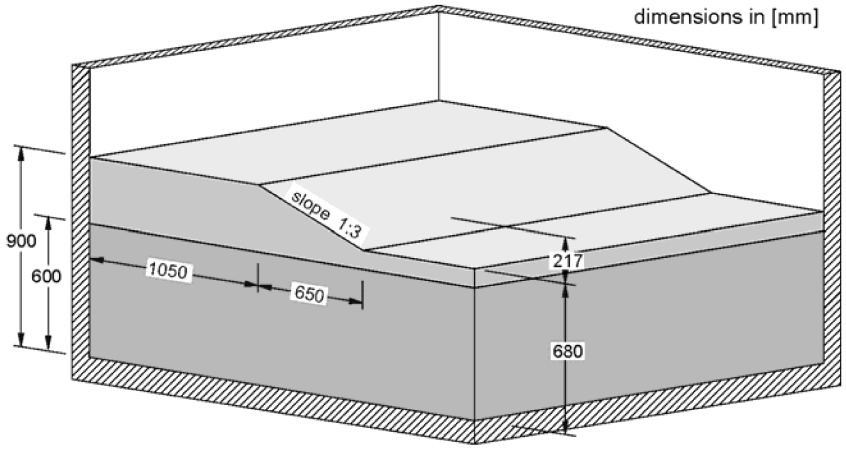

Figure 5: Perspective diagram of the model sloping bank in the test pit

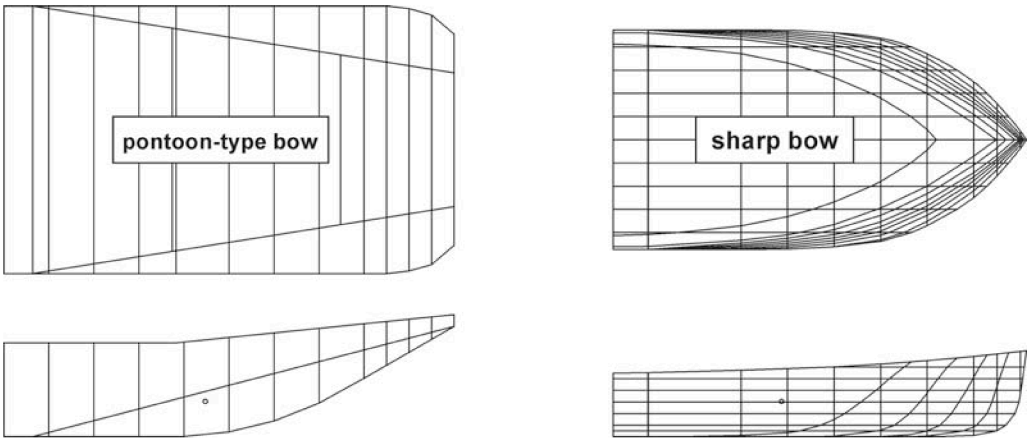

Figure 6: Pontoon-type bow of a type II a Europe barge and the sharp bow of the Johann Welker type of vessel

In the model, the ships were only reproduced up to their centres of gravity owing, inter alia, to the limited amount of space available in the small test pit. However, exact copies of the outer form of the types of bow being investigated were built (Figure 7).

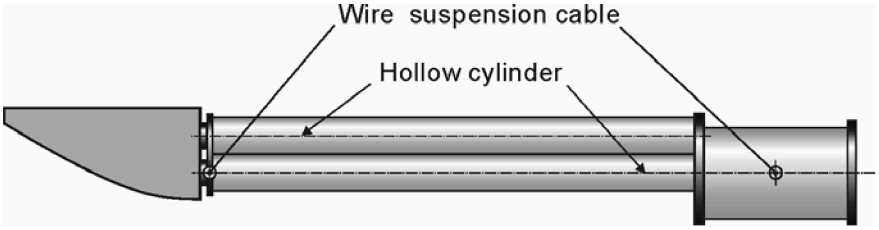

Figure 7: Model of a ship with a pontoon-type bow

The collision was performed as a dynamic action during which it was possible to measure the inertia occurring at the ship and in the soil. To perform the tests, the ships were suspended from two wire cables to form a pendulum. The suspension at the bow of the model included springs dimensioned in such a way that the contact force occurring on collision and when the bow is lifted corresponded exactly to that which occurs when a buoyant ship collides with a sloping bank. To reproduce a ship collision, the ship model suspended on the pendulum was pulled back far enough to allow the collision velocity of the ship required for the test to be achieved when the ship swung back to hit the model slope. The path, velocity and acceleration of the ship and the force were measured during the impact. The pressures and accelerations in the soil were also recorded.

The tests that were performed and the test parameters are summarised in Table 1. Further model tests with other boundary conditions were also performed but are not reported here.

Table 1: Model tests and test parameters

Type of test (Number of tests)	Scale of model	Test parameters
Model tests with a pontoon-type bow (9)	1:23	Velocity on collision: v_a = 0 – 1.16 m/s, Slope inclinations: 1:1, 1:2, 1:3, Mass: m = 191 kg
Model tests with a sharp bow (5)	1:23 1:17.8	Velocity on collision: v_a = 0 – 1.16 m/s, Slope inclination: 1:3, Mass: m = 191 kg

2.2.2. Selected test results

The measured displacements in the directions x and z allow the paths of selected points of the ships to be described. The path of the first point of contact between the bow and the slope is shown in Figure 8 for a typical test performed with a pontoon-type bow and a sharp bow. The paths of both types of bow exhibit characteristic differences. The sharp bow initially penetrates the slope horizontally by around 70 mm. The vertical component of the soil resistance then lifts the sharp bow so that it penetrates the slope further on a path with an inclination that is considerably smaller than that of the slope. By contrast, the pontoon-type bow only penetrates the slope horizontally by 20 mm in the initial phase owing to its blunt form. In the second phase, the ship travels up the sloping bank along a line running almost parallel to the slope until it again penetrates the bank noticeably in the third phase when a horizontal displacement of around 300 mm occurs.

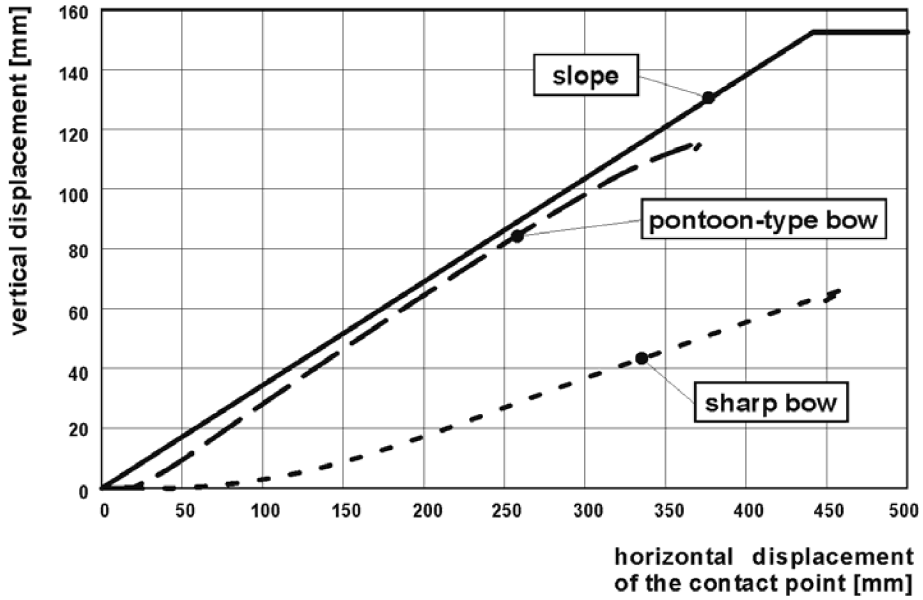

Figure 8: Path of the initial point of contact between the sloping bank and the ship for a pontoon-type bow and a sharp bow

The development of the horizontal component, F_x, of the contact force between the ship's bow and the sloping bank is shown in Figure 9 as a function of the horizontal displacement, s_x, of the point of contact. There are also marked differences in the way the impact force develops. Owing to the large width and the blunt shape of the pontoon-type bow, a significant degree of resistance can develop in the sloping bank in front of the bow right at the beginning of the collision. This resistance results in a pronounced force peak at the very beginning of the collision. The soil resistance, which acts as an impact, deflects the ship so that its bow does not penetrate the slope any further in the second phase but instead slides up the slope along a line running almost parallel to it. At the same time, the contact force continues to increase. After the ship has travelled far enough up the slope, the soil may again fail owing to the increase in the contact force in a third phase. The bow will then penetrate the slope again. Compared with the pontoon-type bow, the contact force increases more or less continuously for a sharp bow until the ship comes to a halt. The sharp bow penetrates the slope and the passive resistance of the soil that increases with the degree of penetration develops on both sides of the bow so that the contact force increases continuously. The two phases of the path of the sharp bow can be clearly identified in the force-displacement graph (Figure 9). In the first phase, in which the bow penetrates the slope horizontally by up to around 70 mm, the force-displacement curve is far steeper than in the second phase in which the path rises.

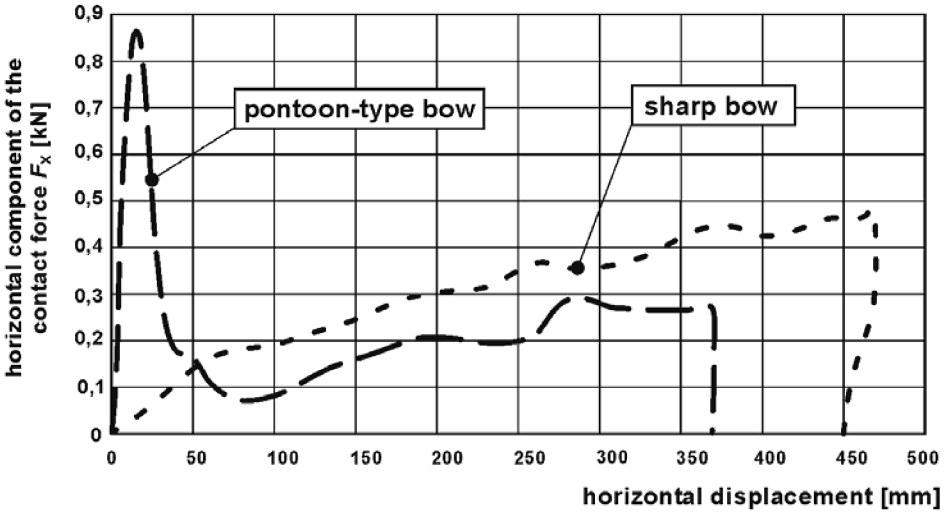

Figure 9: Horizontal component of the contact force as a function of the horizontal displacement for a pontoon-type bow and a sharp bow

2.2.3. Comparison of the test and the theoretical forecast for a pontoon-type bow

The model tests conducted with a pontoon-type bow for a slope with a gradient of 1:3 have shown that the stopping distance is mainly determined by the second phase in which the bow travels up the sloping bank along a line running parallel to it. It would therefore seem obvious to compare the stopping distance determined for the pontoon-type bow in the test with the results of theoretical models in which a rigid slope is assumed ($\alpha = \beta$), i.e. the method according to MEIER-DÖRNBERG and the law of conservation of energy. In both models, the small degree to which the bow penetrates the slope in the first phase is disregarded. A sloping bank with an inclination, α, of 18.3° (1:3) and a friction coefficient between the soil and the hull, $\tan\delta$, of 0.625 ($\delta = 32°$) were assumed for the forecasts. The friction coefficient is the value obtained for the model sand and the hull in the tests.

The maximum horizontal displacements, i.e. the stopping distances, $s_{x,max}$, are shown as a function of the velocity on collision, v_a, in Figure 10. A linear relationship between the stopping distance and the velocity on collision is obtained both by the method according to MEIER-DÖRNBERG and when applying the law of energy conservation. The graph shows that the values of the displacements obtained by the method according to MEIER-DÖRNBERG are slightly lower than the test results. The stopping distances obtained with the law of energy conservation are greater than those obtained for the method according to MEIER-DÖRNBERG as the energy loss on impact in the first phase is not taken into consideration. On the whole, there is a good correlation between the theoretical and experimental stopping distances.

The stopping distance obtained by the method according to MEIER-DÖRNBERG, on which the safety clearance currently required on federal waterways is based, is also shown in Figure 10. A smaller friction coefficient between the ship and the sloping bank, tan δ, of 0.40 ($\delta = 21.8$ °) was assumed in this case in order to obtain a conservative value of the stopping distance. It can be seen that these displacements are greater than the measured displacements. Therefore, the safety clearance for slope inclinations equal to or smaller than 1:3 can also be safely applied to non-rigid slopes.

A comparison of the maximum horizontal contact forces that the ship exerts on the slope at the end of the collision is shown in Figure 11. The forecasts according to MEIER-DÖRNBERG and the law of energy conservation result in a linear correlation between the contact force and the velocity on collision for rigid slopes. Unlike the theoretical forecasts, the development in the model tests is sublinear. This is because higher velocities on collision result in longer stopping distances and a larger degree of upward motion and thus in greater contact forces. The soil cannot withstand these forces and fails. The mean path of the ship in the test is not as steep as stated in the forecast for a rigid slope (Figure 8). The bow is therefore always lifted to a lesser extent in the tests than in a forecast in which a rigid slope is assumed. The horizontal component, F_x, of the contact force is therefore also smaller in the test than in the forecast.

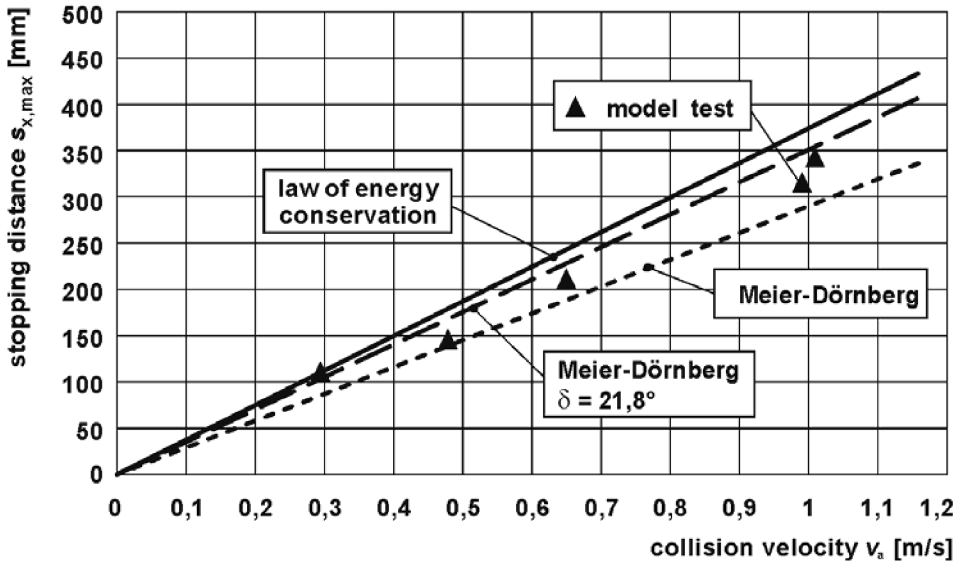

Figure 10: Stopping distance, $s_{x,max}$, as a function of the velocity on collision, v_a, in model tests performed with a pontoon-type bow

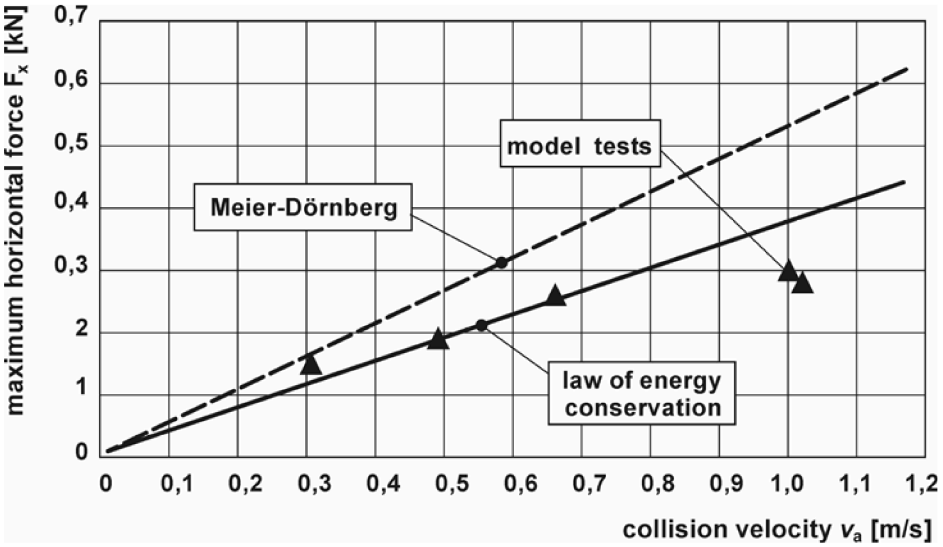

Figure 11: Horizontal component, $F_{x,max}$, of the contact force at the end of the stopping distance as a function of the velocity on collision, v_a, for a ship with a pontoon-type bow

2.3. Field tests

2.3.1. Test set-up

In addition to the model tests, three field tests with the barge *Gerda* were performed on the Elbe-Havel Canal in April 1995. Three collisions took place at right angles and at different velocities and draughts. The ship has a length of 67 m and a width of 8 m and its mass is approximately 900 t at a draught of 1.9 m and 160 t at a draught of 0.6 m. The collisions took place at a 12 m wide embankment (Figure 12) comprising gravel and sand of medium strength which had been specially constructed for the test. The inclination of the embankment was 1:3. The free-board was around 1 m.

The accelerations at the ship and the water pressures beneath the bow of the ship during the collisions were measured. The pore water pressures, the earth pressures and the velocities of ground motion occurring in the slope during the collision were also determined.

Figure 12: Test slope in the field test

2.3.2. Test results

The vertical and horizontal displacements of the point of contact for test no. 2 are shown in Figure 13 and the vertical and horizontal components of the contact force are plotted against time in Figure 14. The collision lasted around 2.4 s, after which the displacements of the point of contact reached their final values of 3.83 m in a horizontal direction ($s_{x,max}$) and 0.85 m in a vertical direction ($s_{z,max}$). Compared with the model tests with a sharp bow, two differences are striking. First, the vertical component of the contact force exhibits a pronounced impact at the start, which can be attributed to the very full shape of the bow of the *Gerda*. It should also be noted that the horizontal component of the contact force decreases after around 1.5 s although the vessel is subsequently lifted a further 0.3 - 0.4 m and a further increase in the horizontal component of the contact force would therefore be expected to occur for structural reasons. The decrease in the horizontal force is probably due to the effect of inertia caused by the vertical acceleration of the bow.

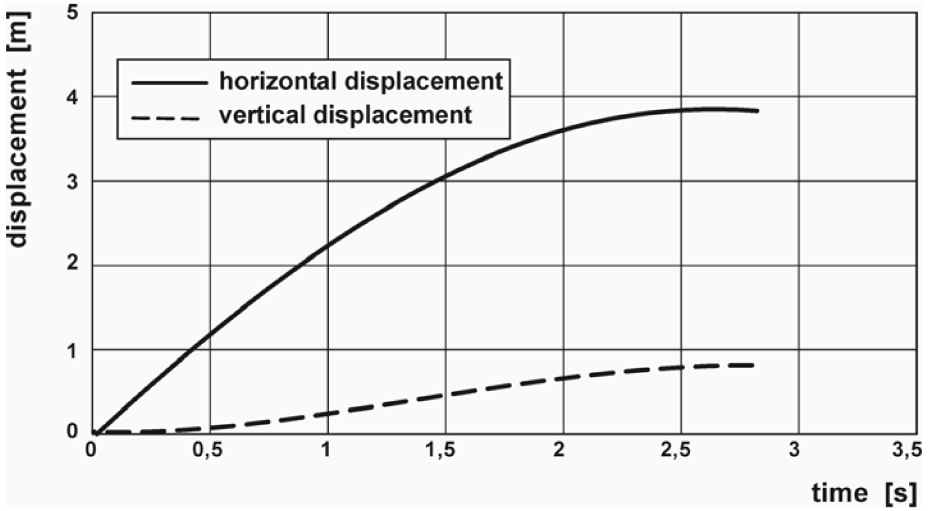

Figure13:Vertical and horizontal displacement of the point of contact in field test no. 2

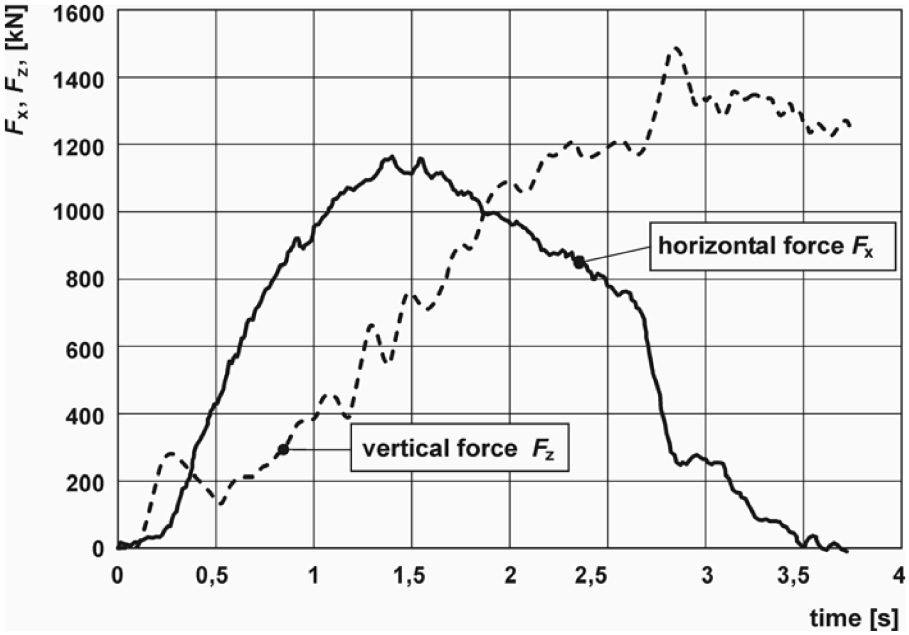

Figure 14: Vertical and horizontal component of the contact force in field test no. 2

2.3.3. Comparison of the field test (Gerda) with the theoretical forecasts

The geometry of the bow of the *Gerda* had to be simplified for the collision forecast. The rounded bow was modelled with two inclined surfaces. A soil wedge due to the passive soil resistance developed at each surface. An angle of friction, φ', of 35° and a mean weight density, γ' (earth-moist and at buoyancy), of 14.6 kN/m² were taken for the gravel and sand of the embankment after penetration tests had been conducted. An angle of friction, δ, of 32°, which had been determined previously in specially designed shear tests, was taken for the friction between the gravel and sand and the steel of the ship's hull. Pore water pressure beneath the bow was not taken into account. The forecast of the stopping distance is based on the law of energy conservation referred to in section 2.2.

A hydrodynamic mass of 10 % of the ship's mass was also included in the calculation of the kinetic energy of the ship.

$$E_{kin} = 1.1 \cdot m_{ship} \cdot v^2/2 = 1.1 \cdot 900 \cdot 2.57^2/2 = 3269 \quad \text{kNm}$$

The mean width, B, and length, L, of the rectangular parallelepiped of the ship's hull used to determine the vertical contact force, F_z, with equation (6) was calculated roughly from the mass of the ship, m_{ship}, a draught, h_0, of 1.90 m and the density of the water using the relationship:

$$m_{ship} = B \cdot L \cdot h_0 \cdot \rho_W$$

$$B \cdot L = \frac{m_{ship}}{h_0 \cdot \rho_W}$$

The deformational work, E_{Ep}, of the passive earth pressure of the soil as a function of the depth to which the ship penetrates the sloping bank is shown in Figure 15, the graph being plotted for the case in which the path of the point of contact between the bow and the bank is horizontal, i.e. the entire kinetic energy of the ship is consumed by the work of the passive resistance of the soil, E_{Ep}. Details on the calculation of the work of the passive resistance of the soil are given in SCHUPPENER ET.AL. (2005).

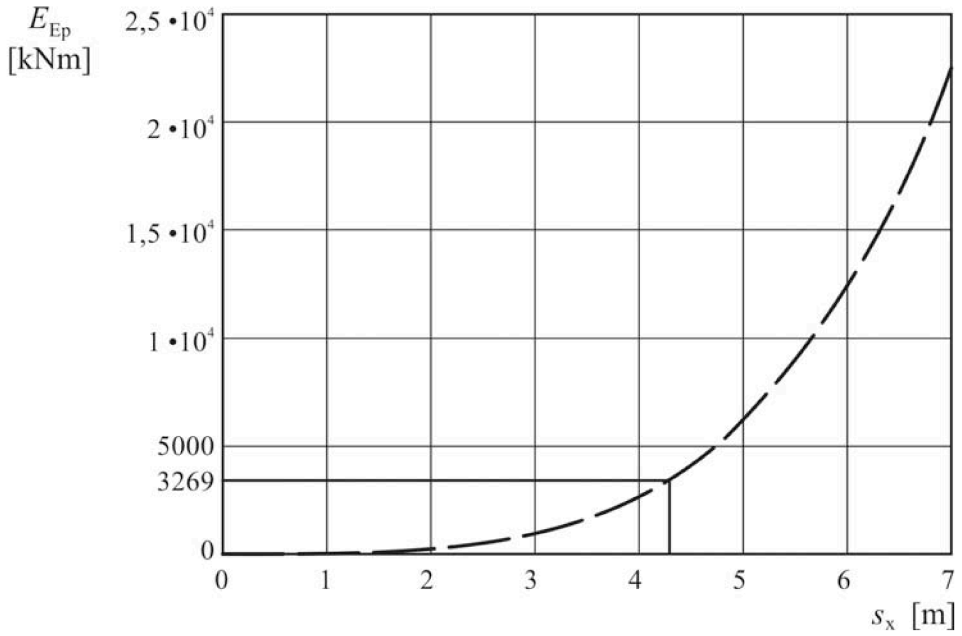

Figure 15:Deformational work E_{Ep} of the passive earth pressure as a function of the horizontal penetration depth s_x

The field tests carried out with the *Gerda* had shown that the bow did not penetrate the slope horizontally but on a path with a mean inclination of 12.4°. A stopping distance with the observed inclination, β, of 12.4° was investigated in a second calculation. In addition to the kinetic energy and the work of the passive resistance of the soil, the potential energy and the frictional work of the contact force at the bow were taken into account in the energy balance. On the basis of these assumptions, the work of the passive resistance of the soil, E_{Ep}, is reduced to 495 kNm, i.e. to less than 15 % of the total kinetic energy. This demonstrates clearly that the geometry of the bow need not be modelled with a particularly great degree of accuracy in order to determine the passive resistance of the soil. In addition, the stopping distance was computed on the basis of the assumption that the slope is rigid, i.e. the ship's bow does not penetrate the slope but slides up its upper surface $(\alpha = \beta)$. The results of the field test and the theoretical forecasts are summarised in Table 2.

The summary in Table 2 shows that there is a good overall correlation between the two forecasts and the results of the field test, both for the contact forces and for the stopping distances:

- The forecasts based on the inclination of the stopping distance, β, of 12.4° observed in the field test yield stopping distances that are between 10 % and 20 % greater than in the test. The forecasts are thus on the safe side.
- The forecasts in which the inclination of the stopping distance is assumed to be the same as the inclination of the slope $(\alpha = \beta)$ underestimate the stopping distance and are therefore not on the safe side.
- The stopping distances forecast with the law of energy conservation always exceed those obtained with the method according to MEIER-DÖRNBERG, as was the case in the model tests. This can partly be explained by the fact that the loss of energy during the deflecting impact at the beginning of the collision is disregarded when the law of energy conservation is applied.

Excess pore water pressures were measured in the soil of the embankment during the collisions in the field tests. However, it was assumed in the forecasts of the stopping distance that no significant excess pore water pressures acted between the bow and the slope and that the contact force could therefore be fully utilised to mobilise friction. The fact that the stopping distance calculated when it is assumed that the friction is fully mobilised is greater than that observed in the field test indicates that there were indeed no significant excess pore water pressures acting directly between the bow and the slope. The measured stopping distances would otherwise have been greater than the distances that had been forecast.

- The forecasts in which the inclination of the stopping distance is assumed to be the same as the inclination of the slope $(\alpha = \beta)$ underestimate the stopping distance and are therefore not on the safe side.
- The stopping distances forecast with the law of energy conservation always exceed those obtained with the method according to MEIER-DÖRNBERG, as was the case in the model tests. This can partly be explained by the fact that the loss of energy during the deflecting impact at the beginning of the collision is disregarded when the law of energy conservation is applied.

Excess pore water pressures were measured in the soil of the embankment during the collisions in the field tests. However, it was assumed in the forecasts of the stopping distance that no significant excess pore water

pressures acted between the bow and the slope and that the contact force could therefore be fully utilised to mobilise friction. The fact that the stopping distance calculated when it is assumed that the friction is fully mobilised is greater than that observed in the field test indicates that there were indeed no significant excess pore water pressures acting directly between the bow and the slope. The measured stopping distances would otherwise have been greater than the distances that had been forecast.

Table 2: Comparison of the stopping distances in the field tests (*Gerda)* and the results of the theoretical forecasts

		Maximum contact force [kN]		Stopping distance [m]	
		horizontal F_x	vertical F_z	horizontal $s_{x,max}$	vertical $s_{z,max}$
Results of field tests:		1200	1500	3.83	0.85
Law of energy conservation	Horizontal stopping path: $\beta = 0°$ (passive soil resistance only)	3000	0	4.27	0
	Inclined stopping path as in field test: $\beta = 12.4°$ (with passive soil resistance)	1623	1220	4.63	1.03
	Inclined stopping path as in field test: $\beta = 12.4°$ (without passive soil resistance)	1276	1303	5.02	1.10
	Inclination of stopping path equal to inclination of slope: $\alpha = \beta = 18.4°$	1733	1434	3.63	1.21
MEIER-DÖRNBERG	Inclined stopping path as in field test: $\beta = 12.4°$	1299	1326	4.2	0.93
	Inclination of stopping path equal to inclination of slope: $\alpha = \beta = 18.4°$	1610	1351	3.1	0.99

3. SUMMARY AND OUTLOOK

The stopping distance of a ship during a collision with a sloping bank on a waterway and the loads occurring during that collision can be determined theoretically by applying the principle of linear momentum and the principle of the conservation of angular momentum for a fully plastic impact according to MEIER-DÖRNBERG (1983) and the energy conservation law. Model tests and field tests, in which the degree to which inland navigation craft with typical bow designs penetrate and travel up a sloped bank were investigated, have been performed by the Federal Waterways Engineering and Research Institute in recent years. A comparison of the observed soil-mechanical failure mechanisms, stopping distances and forces with the models of the forecasts shows that there is a satisfactory correlation between them which will enable the models of the forecasts to be applied under other boundary conditions during collisions as well as to collisions by ocean-going vessels.

For nautical reasons, ship collisions generally occur when a ship is approaching a bank at an oblique angle, ε, of less than 30°. In this case, the ship does not continue its journey in a straight line but is pushed back down into the water by the contact force that acts laterally. Upon collision with a rigid slope, the bow therefore describes a curved path and slides back down the slope after reaching its highest point. To find out whether the bow of the ship would reach a bridge abutment, the stopping distance can be estimated conservatively by assuming that the collision is perpendicular to the slope and by selecting the angle that results for a linear collision path on a rigid slope at a collision angle, ε, as the inclination, β, of the collision path (Figure 16, left).

In order to take account of the penetration of the slope by a pontoon-type bow, which occurs for geometrical reasons when a vessel approaches the sloping bank at an oblique angle, it can be assumed that the bow penetrates owing to a continuous failure of the ground caused by the contact force acting on the slope. To enable a relationship between the load at ground failure and the penetration of the bow to be formulated, it is assumed that the ship initially rests on the edge of the bow. The side of the ship rises nearly vertically on one side of the edge of the bow while the virtually horizontal surface of the pontoon-type bow is adjacent to it on the other side (see Figure 16, right). Under these conditions, the following relationship is obtained between the perpendicular penetration, z_{Gb}, of the bow of the ship, the inclination of the slope, ν, at right angles to the collision path and the width, b_{Gb}, supporting the edge of the bow:

$$z_{Gb} = b_{Gb} \cdot \tan \nu \qquad (14)$$

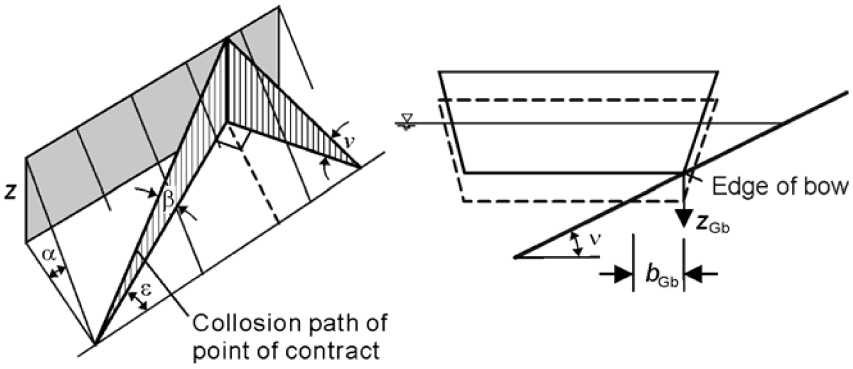

Figure 16: Geometrical relationships for a collision at an oblique angle and penetration of the sloped bank

Furthermore, it is assumed that the ground failure load corresponds to the vertical component of the contract force, F_z, which is evenly distributed over the length of the slope supporting the edge of the bow. The vertical ground pressure, σ_{Gb}, on ground failure can be determined for an infinitely long linear load as a function of the width, b_{Gb}, supporting the edge of the bow and depends on the soil parameters and the slope inclination, ν, at right angles to the collision path. The contact force, taken as the ground failure load, is then:

$$F_z = \sigma_{Gb}(b_{Gb}) \cdot s_{x,max} \cdot b_{Gb} \qquad (15)$$

The vertical component, z_{Gb}, of the penetration of the bow can then be calculated iteratively with equations (14) and (15). As it is assumed that the bow penetrates the slope, the inclination, β, selected for the collision path should be several degrees smaller for the calculation of the contact force, F_z, and the stopping distance, $s_{x,max}$, than when a rigid slope is assumed (Figure 17). It must subsequently be checked whether the calculated vertical penetration of the ship's bow, z_{Gb}, corresponds to the inclination, β, of the collision path chosen initially. If the calculated penetration of the bow is too great, the inclination selected for the collision path was too steep. By contrast, the assumed inclination of the collision path was too small if the calculated penetration of the bow is less than that obtained for the assumed inclination of the collision path (Figure 17).

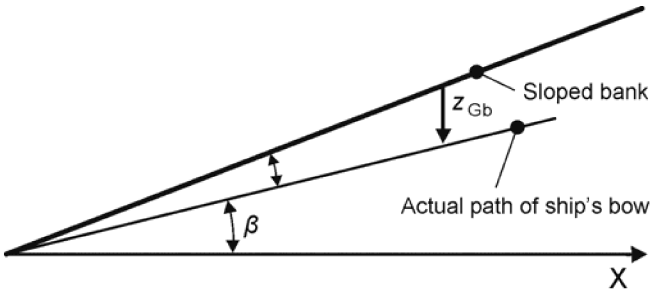

Figure 17: Sloped bank, perpendicular penetration of the ship's bow and actual path of the ship's bow on penetrating the slope

For the sake of completeness, the deformational work due to the ground failure in the sloped bank can also be taken into account in the iteration, as follows:

$$E_{Gb} = ½ \cdot N \cdot z_{Gb}.$$

4. BIBLIOGRAPHY

Calgaro, J.A., Chocs de bateaux contre les piles de pont, Juin 1991, Ministre de l'équipement, du logement, des transports et de la mer

Denver, H., Design of protective islands by means of geotechnical model tests, Geotechnical Report No. 12, Danish Geotechnical Institute, 1983

DIN 1055 Part 9 (2003-08), Actions on structures – Accidental actions

Meier-Dörnberg, K. E., Schiffskollisionen, Sicherheitszonen und Lastannahmen für Bauwerke an Binnenwasserstraßen, Kurz-Veröffentlichung im VDI-Bericht Nr. 496, 1983.

Schuppener, B., Kauther, R., Kramer, H., Vorbau, J., Schiffsanfahrungen an Uferböschungen, 1. Hans Lorenz Symposium des Grundbauinstitutes der TU Berlin am 13. Oktober 2005